

# $\phi$ Meson Production in Small Collision Systems

M. M. Mitrankova<sup>a,\*</sup>, Yu. M. Mitrankov<sup>a</sup>, D. O. Kotov<sup>a</sup>, Ya. A. Berdnikov<sup>a</sup>, and A. Ya. Berdnikov<sup>a</sup>

<sup>a</sup> Peter the Great St. Petersburg Polytechnic University, St. Petersburg, 195251 Russia

\*e-mail: mashalario@gmail.com

Received March 11, 2021; revised July 8, 2021; accepted July 18, 2021

**Abstract**—Production of  $\phi$  mesons in small collision systems at  $\sqrt{s_{NN}} = 200$  GeV has been studied in the PHENIX experiment at the RHIC. The  $\phi$  meson nuclear modification factors have been investigated in the following collision systems:  $p + \text{Al}$ ,  $p + \text{Au}$ ,  $d + \text{Au}$ , and  ${}^3\text{He} + \text{Au}$ . The  $\phi$  meson nuclear modification factors have been compared with the  $\pi^0$  meson nuclear modification factors in  $p + \text{Al}$  and  ${}^3\text{He} + \text{Au}$  collisions and the  $\phi$ ,  $\pi^0$  meson nuclear modification factors have been compared with the nuclear modification factors  $(p + \bar{p})/2$  in the  $p + \text{Au}$  collisions.

DOI: 10.1134/S1063779622020563

## INTRODUCTION

Quantum chromodynamics predicts a state of matter (quark–gluon plasma, QGP), in which quarks and gluons are in the unbound state [1]. Collisions of heavy ions provide a unique possibility for studying the properties and characteristics of QGP under laboratory conditions, which is the main purpose of the PHENIX experiment [2].

One of the ways for determining the characteristics of strongly interacting hot and dense matter (QGP), formed in collisions of ultrarelativistic heavy ions, is the study of the parton energy loss in this matter by investigating the production of hadrons. The parton energy loss in QGP can be found by suppressing the production of hadrons with large transverse momentum  $p_T$  in collisions of heavy ions in comparison with proton–proton collisions (the so-called jet quenching effect [3]). Another evidence of QGP formation is the enhanced yield of strangeness in collisions of relativistic ions in comparison with elementary proton–proton collisions, which manifests itself as an excess production of hadrons, containing  $s$  and  $\bar{s}$  quarks. Excess production of strange particles in high-energy collisions of heavy ions in comparison with  $p + p$  collisions is a direct consequence of the process of chemical equilibrium of strange quarks in QGP [4].

The QGP properties can be studied experimentally by measuring the yields of final state particles. Vector  $\phi$  meson has a small collisional cross section with non-strange hadrons and its lifetime ( $42 \text{ fm s}^{-1}$ ) [5] is much larger than the QGP lifetime ( $\sim 5 \text{ fm s}^{-1}$ ) [6]. Due to these properties,  $\phi$  meson production is less affected by hadronic collisions at the late evolution stage of the system, formed in collisions of heavy nuclei, and its daughter particles do not rescatter in the hadronic

phase. Measurement of the  $\phi$  meson yield is used for studying both the dependence of the jet quenching effect on the quark composition of produced particles and enhanced strangeness yield in collisions of relativistic ions, because the  $\phi$  meson is the lightest bound state of  $s$  and  $\bar{s}$  quarks and can be measured in the range of large transverse momenta [5]. It should also be noted that the mass of  $\phi$  meson ( $1019.46 \pm 0.02 \text{ MeV } c^{-2}$  [7]) is comparable with that of the lightest baryons (e.g., proton), which makes it possible to study the hadron production processes depending on flavor, quark number, and mass of produced particles.

Study of the fluxes of different orders in collisions of small systems ( $p + \text{Au}$ ,  $d + \text{Au}$ ,  ${}^3\text{He} + \text{Au}$ ) suggests that, contrary to expectations, QGP can be formed in these collisions [8]. If so, one will be able to find evidence of the energy loss in plasma, manifesting itself in the specific features of hadron production.

Study of small systems can also help to interpret the results of light hadron production in collisions of heavy ions (in particular, the observed difference between nuclear modification factors of  $\pi^0$ ,  $\phi$  mesons and  $(p + \bar{p})/2$ , which were obtained in  $\text{Au} + \text{Au}$ ,  $\text{Cu} + \text{Cu}$ , and  $\text{Cu} + \text{Au}$  collisions at  $\sqrt{s_{NN}} = 200$  GeV and in  $\text{U} + \text{U}$  collisions at  $\sqrt{s_{NN}} = 192$  GeV [9, 10].

## MEASURING PROCEDURE

The experimental data on  $p + \text{Al}$  and  $p + \text{Au}$  interactions were obtained in the PHENIX experiment in 2015 and the data on  ${}^3\text{He} + \text{Au}$  interactions were obtained in 2014 at an energy  $\sqrt{s_{NN}} = 200$  GeV in the low rapidity range ( $|\eta| < 0.35$ , where  $\eta$  is the pseudorapidity).

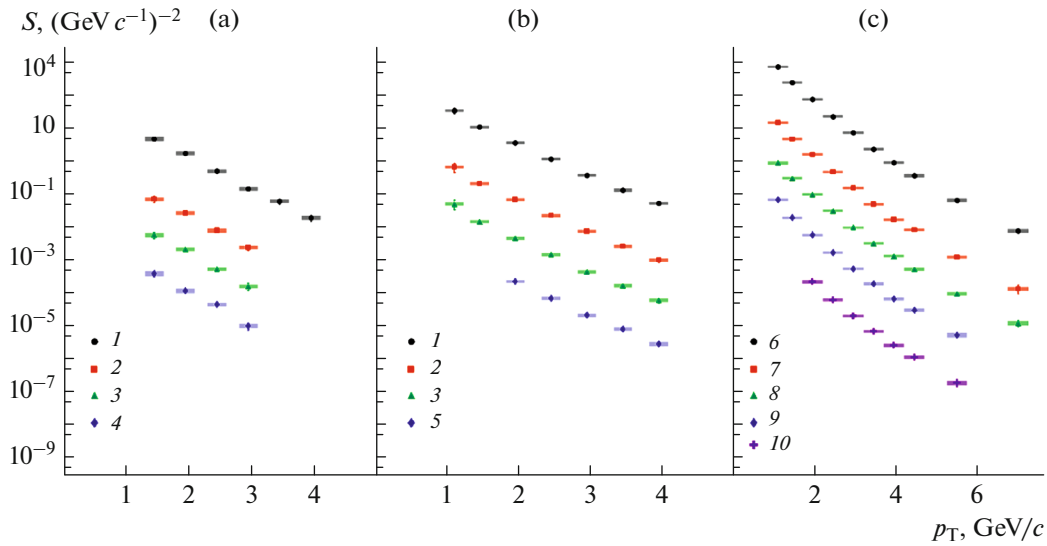


**Fig. 1.** Invariant transverse momentum spectra  $S$ , measured for  $\phi$  mesons in (a)  $p + \text{Al}$ , (b)  $p + \text{Au}$ , and (c)  ${}^3\text{He} + \text{Au}$  collisions at  $\sqrt{s_{NN}} = 200$  GeV in the low rapidity range. The measurements were performed for the following centrality classes of events: (1)  $0\text{--}72(84)\% \times 10^4$ , (2)  $0\text{--}20\% \times 10^2$ , (3)  $20\text{--}40\% \times 10^1$ , (4)  $40\text{--}72\% \times 10^0$ , (5)  $40\text{--}84\% \times 10^0$ , (6)  $0\text{--}88\% \times 10^5$ , (7)  $0\text{--}20\% \times 10^3$ , (8)  $20\text{--}40\% \times 10^2$ , (9)  $40\text{--}60\% \times 10^1$ , and (10)  $60\text{--}88\% \times 10^1$ , plotted for clarity with the corresponding factors. Hereinafter, error bars and rectangles denote statistical and systematic errors, respectively.

Electrons, charged hadrons, and photons are detected in two central spectrometric arms (east and west ones) of the PHENIX detector. In this analysis, drift chambers were used, which determine the momentum of charged particles and a BBC detector, designed to determine the collision centrality [2].

One cannot distinguish between kaons, produced in the decay of a  $\phi$  meson, and other kaons; therefore, all tracks of charged particles from each event are combined into pairs with opposite charges. All charged particles are assumed to be kaons; therefore, the kaon mass is assigned to them. The components of the 3-momentum vector of each track are determined using a drift chamber, based on which the invariant mass and transverse momentum for a kaon pair are calculated according to the two-particle decay kinematics.

Along with the useful signal of  $\phi$  mesons, the distribution over invariant mass for a pair of kaons with the opposite signs contains a combinatorial background, consisting of the correlated and uncorrelated components. The uncorrelated background was estimated according to the mixed events method [11]. After subtraction of the uncorrelated background from the general spectrum, the signal and the correlated background of the distribution over the invariant mass were approximated by a convolution of a Breit–Wigner function with a Gaussian function and by a polynomial function, respectively. The dispersion of the Gaussian function, which is interpreted as the mass resolution of the detector, and the efficiency of

$\phi$  mesons reconstruction were determined using the complete simulation of the PHENIX detector in the GEANT code package [12] with zero width  $\phi \rightarrow K^+K^-$ , in which the  $\phi$  meson has an infinite lifetime. Yields of  $\phi$  mesons were calculated by integrating the distribution over the invariant mass in the range of  $\pm 9$  MeV  $c^{-2}$  near the mass of the  $\phi$  meson ( $1.019$  GeV  $c^{-2}$ ) after subtraction of the combinatorial background.

## RESULTS AND DISCUSSION

Figure 1 shows the invariant spectra over the transverse momentum  $S = \frac{1}{2\pi p_T} \frac{d^2N}{dp_T dy}$  ( $y$  is rapidity and  $N$  is the number of  $\phi$  mesons, recorded by the experimental setup (meson yield) [13]) in  $p + \text{Al}$ ,  $p + \text{Au}$ , and  ${}^3\text{He} + \text{Au}$  collisions at  $\sqrt{s_{NN}} = 200$  GeV in the low rapidity range ( $|\eta| < 0.35$ ).

The measurements were performed in the transverse momentum range from 1.1 to 3.95 GeV  $c^{-1}$  for four centrality classes of events in  $p + \text{Al}$  and  $p + \text{Au}$  collisions and in the range from 1.1 to 7.0 GeV  $c^{-1}$  for five centrality classes of events in  ${}^3\text{He} + \text{Au}$  collisions. The values of the invariant spectra of  $\phi$  mesons are used to calculate the nuclear modification factors [13].

The nuclear modification factors  $R_{AB}$  [13], measured for  $\phi$  mesons in  $p + \text{Al}$ ,  $p + \text{Au}$ ,  $d + \text{Au}$ , and  ${}^3\text{He} + \text{Au}$  collisions at  $\sqrt{s_{NN}} = 200$  GeV at different

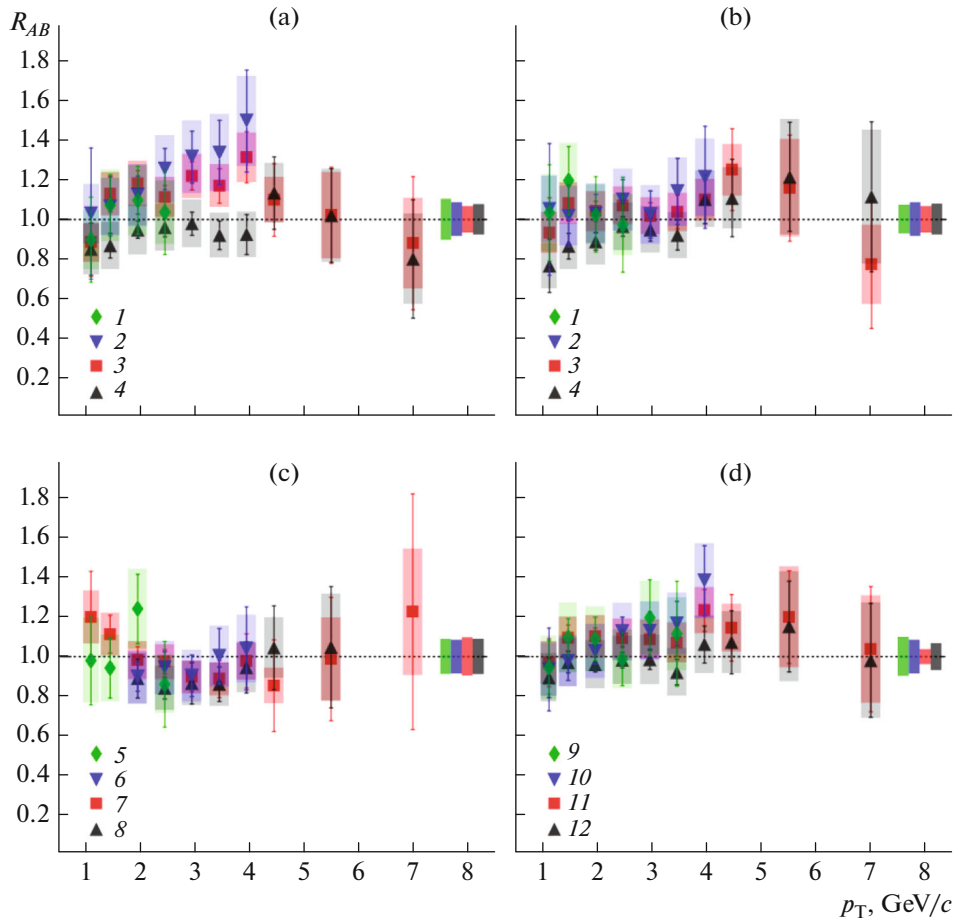


**Fig. 2.** Comparison of the nuclear modification factors of  $\phi$  mesons in (1)  $p + \text{Al}$ , (2)  $p + \text{Au}$ , (3)  $d + \text{Au}$ , and (4)  ${}^3\text{He} + \text{Au}$  collisions at  $\sqrt{s_{NN}} = 200$  GeV for four centrality classes of events ((a) 0–20%; (b) 20–40%; (c) (5) 40–72%  $p + \text{Al}$ , (6) 40–84%  $p + \text{Au}$ , (7) 60–88%  $d + \text{Au}$ , and (8) 60–88%  ${}^3\text{He} + \text{Au}$ ; and (d) (9) 0–72%  $p + \text{Al}$ , (10) 0–84%  $p + \text{Au}$ , (11) 0–88%  $d + \text{Au}$ , and (12) 0–88%  ${}^3\text{He} + \text{Au}$ ) in the low rapidity range. The systematic uncertainty, related to the uncertainty of the number of binary nucleon–nucleon collisions, is indicated by the rectangles on the right.

collision centralities are shown in Fig. 2. In all centralities, the  $R_{AB}$  values for  $\phi$  mesons are unity in the entire transverse momentum range within the measurement uncertainty.

The nuclear modification factors of  $\phi$  mesons and  $\pi^0$  mesons in  $p + \text{Al}$  and  ${}^3\text{He} + \text{Au}$  collisions at  $\sqrt{s_{NN}} = 200$  GeV are compared in Figs. 3a and 3c. Fig. 3.

For all centralities and in the entire transverse momentum range, the  $R_{AB}$  values of  $\phi$  mesons and  $\pi^0$  mesons are identical within the measurement uncertainty, which can indicate that no enhanced strangeness yield in small collision systems is observed. This fact can also indicate that the effects of cold nuclear matter do not affect the difference in the  $R_{AB}$  values of  $\phi$  mesons and  $\pi^0$  mesons in  $\text{Au} + \text{Au}$ ,  $\text{Cu} + \text{Cu}$ ,  $\text{Cu} + \text{Au}$ , and  $\text{U} + \text{U}$  collisions [9, 10].

Figure 3b shows the comparison of the nuclear modification factors of  $\phi$  and  $\pi^0$  mesons with the nuclear modification factors  $(p + \bar{p})/2$  in  $p + \text{Au}$  collisions. The nuclear modification factors of light mesons coincide within errors, whereas the nuclear modification factors  $(p + \bar{p})/2$  exceed those of  $\phi$  mesons and  $\pi^0$  mesons. A difference in the nuclear modification factors of  $\phi$  mesons and  $(p + \bar{p})/2$  indicates that production of these hadrons is determined by the quark composition rather than mass of the produced particles. A similar result for  $(p + \bar{p})/2$  was obtained in collisions of heavy ions, whereas the nuclear modification factors of light mesons in collisions of heavy ions differ from the results, which were obtained in small collision systems: yields of  $\pi^0$  mesons are more suppressed than those of  $\phi$  mesons [9].

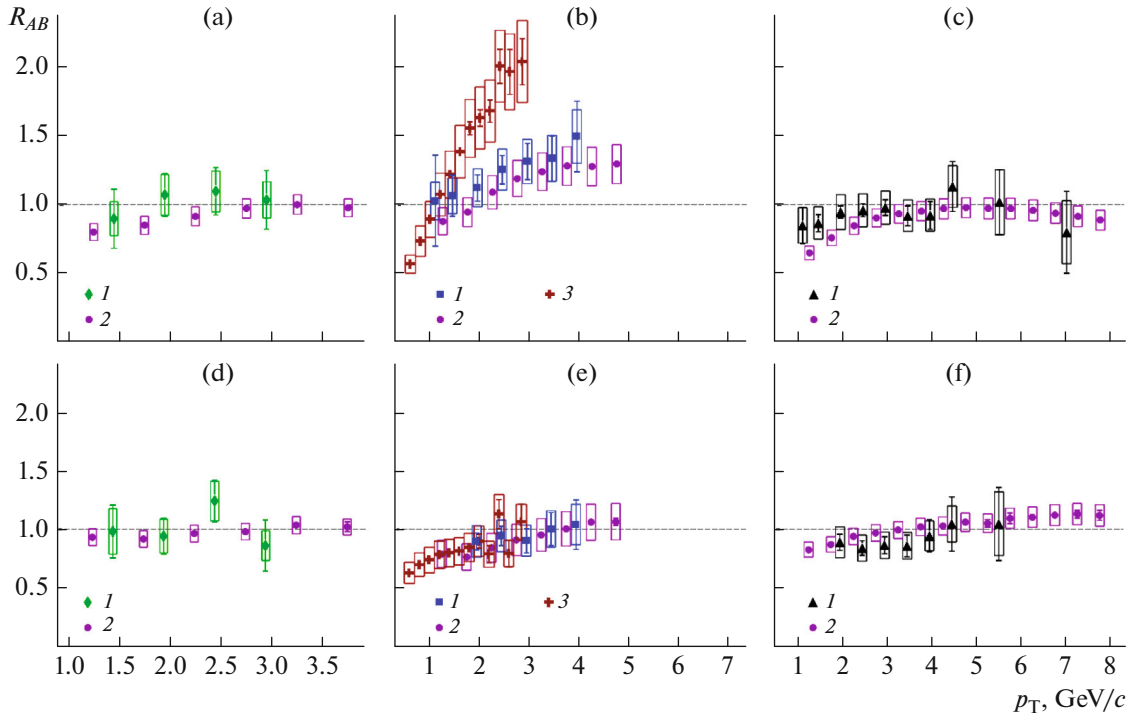


**Fig. 3.** Comparison of the nuclear modification factors of (1)  $\phi$  meson and (2)  $\pi^0$  meson in (a)  $p + \text{Al}$  and (c)  ${}^3\text{He} + \text{Au}$  collisions and of (1)  $\phi$  meson, (2)  $\pi^0$  meson, and (3)  $(p + \bar{p})/2$  in (b)  $p + \text{Au}$  collisions at  $\sqrt{s_{NN}} = 200$  GeV in the low rapidity range.

### CONCLUSIONS

The invariant transverse momentum spectra and nuclear modification factors of  $\phi$  mesons, measured in  $p + \text{Al}$ ,  $p + \text{Au}$ , and  ${}^3\text{He} + \text{Au}$  collisions at  $\sqrt{s_{NN}} = 200$  GeV in the transverse momentum range of  $1.0 < p_T < 4.0$  GeV  $c^{-1}$  in  $p + \text{Al}$  and  $p + \text{Au}$  collisions and in the range of  $1.0 < p_T < 7.0$  GeV  $c^{-1}$  in  ${}^3\text{He} + \text{Au}$  collisions for different centrality classes of events over the kaon decay channel, were presented. In all centralities and in the entire transverse momentum range, the nuclear modification factors of  $\phi$  mesons are unity within the measurement uncertainty. Coincidence of the nuclear modification factors of  $\phi$  mesons and  $\pi^0$  mesons in small systems may indicate that no enhanced strangeness yield is observed in small collision systems and the effects of cold nuclear matter do not affect the difference in the nuclear modification factors of  $\phi$  mesons and  $\pi^0$  mesons in collisions of heavy ions. The nuclear modification factors of  $(p + \bar{p})/2$  exceed those of  $\phi$  mesons and  $\pi^0$  mesons. Different yields of  $\phi$  mesons and  $(p + \bar{p})/2$  indicate that the processes of production of these hadrons are determined by the quark composition rather than mass of the produced particles. Production of  $\phi$  mesons in asymmetric small systems at the RHIC was studied for the first time and the results supplement the results of studying the production of  $\phi$  mesons in

$p + p$  and  $d + \text{Au}$  collisions and in collisions of heavy ions.

### FUNDING

This study was performed within the State assignment for carrying out basic studies (project no. FSEG-2020-0024).

### CONFLICT OF INTEREST

The authors declare that they have no conflicts of interest.

### REFERENCES

1. K. Adcox, et al. (PHENIX Collab.), “Formation of dense partonic matter in relativistic nucleus-nucleus collisions at RHIC: Experimental evaluation by the PHENIX collaboration,” *Nucl. Phys. A.* **757**, 184–283 (2005).
2. K. Adcox, et al. (PHENIX Collab.), “PHENIX detector overview,” *Nucl. Instrum. Methods Phys. Res., Sect. A.* **499**, 469–479 (2003).
3. D. d’Enterria, “Jet quenching,” in *Landolt–Börnstein* (Springer Verlag, 2009), Vol. 23, p. 471.
4. P. Koch, B. Muller, and J. Rafelski, “Strangeness in relativistic heavy ion collisions,” *Phys. Rep.* **142**, 167–172 (1986).
5. A. Shor, “ $\phi$ -meson production as a probe of the quark-gluon plasma,” *Phys. Rev. Lett.* **54**, 1122–1125 (1985).

6. K. Adcox, et al. (PHENIX Collab.), “Formation of dense partonic matter in relativistic nucleus–nucleus collisions at RHIC: Experimental evaluation by the PHENIX collaboration,” *Nucl. Phys. A.* **757**, 184–283 (2005).
7. J. Beringer, et al. (Particle Data Group), “ $\phi(1020)$ ,” *Phys. Rev. D.* **86**, 010001 (2012).
8. C. Aidala, et al. (PHENIX Collab.), “Creation of quark-gluon plasma droplets with three distinct geometries,” *Nat. Phys.* **15**, 214–220 (2019).
9. A. Adare, et al. (PHENIX Collab.), “Nuclear modification factors of  $\phi$ -mesons in  $d + Au$ ,  $Cu + Cu$ , and  $Au + Au$  collisions at  $\sqrt{s_{NN}} = 200$  GeV,” *Phys. Rev. C.* **83**, 024909 (2011).
10. A. Berdnikov, Ya. Berdnikov, D. Kotov, and Yu. Mitrankov, “ $\phi$ -meson measurements in  $Cu + Au$  collisions at 200 GeV and in  $U + U$  collisions at 192 GeV,” *J. Phys.: Conf. Ser.* **1135**, 012044 (2018).
11. S. S. Adler, et al. (PHENIX Collab.), “Production of  $\phi$ -mesons at midrapidity in  $\sqrt{s_{NN}} = 200$  GeV  $Au + Au$  collisions at relativistic energies,” *Phys. Rev. C.* **72**, 014903 (2005).
12. R. Brun, F. Carminati, and S. Giani, *GEANT Detector Description and Simulation Tool* (CERN, Geneva, 1993).
13. A. Berdnikov, Ya. Berdnikov, D. Kotov, et al., “Measuring phi mesons in  $p + Au$  and  $He + Au$  collisions at 200 GeV,” *Bull. Russ. Acad. Sci. Phys.* **84**, 1533 (2020).

*Translated by A. Sin'kov*